Check for updates

Rameez K. Rahman
Center for Advanced Turbomachinery and Energy Research (CATER),
University of Central Florida,
Orlando, FL 32816
e-mail: rameeskr@knights.ucf.edu

Samuel Barak
Center for Advanced Turbomachinery and Energy Research (CATER),
University of Central Florida,
Orlando, FL 32816
e-mail: sambarak@knights.ucf.edu

K.R.V. (Raghu) Manikantachari
Center for Advanced Turbomachinery and Energy Research (CATER),
University of Central Florida,
Orlando, FL 32816
e-mail: raghu@ucf.edu

Erik Ninnemann
Center for Advanced Turbomachinery and Energy Research (CATER),
University of Central Florida,
Orlando, FL 32816
e-mail: erik.ninnemann@Knights.ucf.edu

Ashvin Hosangadi
CRAFT Tech,
Pipersville, PA 18947
e-mail: hosangad@craft-tech.com

Andrea Zambon
CRAFT Tech,
Pipersville, PA 18947
e-mail: azambon@craft-tech.com

Subith S. Vasu[1]
Center for Advanced Turbomachinery and Energy Research (CATER),
University of Central Florida,
Orlando, FL 32816
e-mail: subith@ucf.edu

Probing the Effects of NO_x and SO_x Impurities on Oxy-Fuel Combustion in Supercritical CO_2: Shock Tube Experiments and Chemical Kinetic Modeling

The direct-fired supercritical carbon dioxide cycles are one of the most promising power generation methods in terms of their efficiency and environmental friendliness. Two important challenges in implementing these cycles are the high pressure (300 bar) and high CO_2 dilution (>80%) in the combustor. The design and development of supercritical oxy-combustors for natural gas require accurate reaction kinetic models to predict the combustion outcomes. The presence of a small amount of impurities in natural gas and other feed streams to oxy-combustors makes these predictions even more complex. During oxy-combustion, trace amounts of nitrogen present in the oxidizer is converted to NO_x and gets into the combustion chamber along with the recirculated CO_2. Similarly, natural gas can contain a trace amount of ammonia and sulfurous impurities that get converted to NO_x and SO_x and get back into the combustion chamber with recirculated CO_2. In this work, a reaction model is developed for predicting the effect of impurities such as NO_x and SO_x on supercritical methane combustion. The base mechanism used in this work is GRI Mech 3.0. H_2S combustion chemistry is obtained from Bongartz et al. while NO_x chemistry is from Konnov. The reaction model is then optimized for a pressure range of 30–300 bar using high-pressure shock tube data from the literature. It is then validated with data obtained from the literature for methane combustion, H_2S oxidation, and NO_x effects on ignition delay. The effect of impurities on CH_4 combustion up to 16 atm is validated using NO_x-doped methane studies obtained from the literature. In order to validate the model for high-pressure conditions, experiments are conducted at the UCF shock tube facility using natural gas identical mixtures with N_2O as an impurity at ~100 bar. Current results show that there is a significant change in ignition delay with the presence of impurities. A comparison is made with experimental data using the developed model and predictions are found to be in good agreement. The model developed was used to study the effect of impurities on CO formation from sCO_2 combustors. It was found that NO_x helps in reducing CO formation while the presence of H_2S results in the formation of more CO. The reaction mechanism developed herein can also be used as a base mechanism to develop reduced mechanisms for use in CFD simulations. [DOI: 10.1115/1.4047314]

Keywords: supercritical carbon dioxide, reaction mechanism, shock tube, NO_x, SO_x, high pressure, ignition delay

1 Introduction

Supercritical CO_2 cycles for power generation have received increased attention recently due to the possibilities for zero-emission, high efficiency, and compactness of the turbomachinery components [1–15]. The direct-fired supercritical carbon dioxide (sCO_2) cycles are one of the most promising power generation methods in terms of efficiency [1,16] and can be coupled with both syngas and natural gas fuels. High-pressure carbon dioxide produced during their operation makes carbon capture and sequestration easier making it environmentally friendly. Due to this, direct-fired sCO_2 cycles are an attractive choice for power generation. However, the extreme operating conditions such as high temperature (~1500 K), high pressure (~150–300 bar), and high CO_2 dilution makes the implementation challenges. Additionally, the feed to sCO_2 combustor, natural gas, may contain a small amount of impurities in the form of hydrogen sulfide and ammonia depending on the gas/coal fields and processing facilities they are obtained from. During combustion, these get converted to sulfur oxides (SO_x) and nitrogen oxides (NO_x). Since, a part of combustion exhaust is recirculated in sCO_2 combustors, incoming natural gas feed undergoes combustion in the presence of these impurities. To understand the effect of these extreme conditions and impurities on sCO_2 combustion, systematic experimental and simulation studies are necessary.

Due to the complexity, safety, and cost of experiments, experimental studies on methane combustion at high pressure (>100 bar) and high CO_2 dilution are scarce although many studies exist at lower pressures with CO_2 addition in the literature [3,9,11,13,14,17–24]. Shao et al. [25] conducted ignition delay measurements in a shock tube at 30–300 bar for lean and stoichiometric $CH_4/O_2/CO_2$ and $H_2/O_2/CO_2$ mixtures for a temperature

[1]Corresponding author.

Contributed by the Advanced Energy Systems Division of ASME for publication in the Journal of Energy Resources Technology. Manuscript received April 17, 2020; final manuscript received April 19, 2020; published online June 12, 2020. Editor: Hameed Metghalchi.

Downloaded from http://asmedigitalcollection.asme.org/energyresources/article-pdf/142/12/122302/6543135/jert_142_12_122302.pdf by guest on 28 November 2022

range of 1045–1578 K. They found measured ignition delay times to be shorter with an increase in pressure and pointed out that accurate reaction rate measurements are required for some reactions with large pressure dependency. Barak et al. [15,26] conducted shock tube ignition delay measurements near 100 atm in mixtures of oxy-syngas and oxy-methane added to CO_2 bath gas environments. In total, five mixtures were investigated in their study within a pressure range of 70–100 atm and a temperature range of 1050–1350 K. Another interesting result from this work was that Aramco 2.0 [27] mechanism was able to predict ignition delay for their experiments relatively well. Also, there has been recent work by the current authors on assessing the impact of supercritical CO_2 on combustion using theoretical methods [13,28–37]. However, literature still lacks experimental studies on the effect of impurities on natural gas combustion at sCO_2 combustor relevant conditions.

In this work, an optimized reaction mechanism is developed for sCO_2 combustor conditions using C1–C3, H_2S, and NO_x mechanisms available in the literature. Also, presented herein are the shock tube ignition delay times for natural gas feed containing 1% N_2O at 100 bar and temperature range of 1440–1574 K at an equivalence ratio of 1. To the best of the authors knowledge, this is the first study to report ignition delay capturing an impurity effect in natural gas combustion near 100 bar.

2 Methodology

2.1 Kinetic Modeling and Optimization. To develop a base mechanism for sCO_2 combustion in the presence of impurities, a mechanism that accurately describes: (1) C1–C3 combustion chemistry, (2) H_2S oxidation and pyrolysis chemistry, and (3) NO_x formation chemistry was required.

2.1.1 C1–C3 Chemistry. For CI–C3 chemistry, the GRI 3.0 [38] mechanism was chosen. GRI 3.0 has 53 species and 325 reactions that are well-validated for combustion of natural gas mixtures containing C1–C3 species. GRI 3.0 is validated for methane ignition delay at lean and rich conditions, shock tube species profiles, flow reactor studies, flame speed measurements, and prompt NO under a wide range of conditions. Since the fuels of interest in this work contain mostly methane, GRI 3.0 will be able to capture the combustion process with reasonable accuracy at atmospheric pressure.

2.1.2 H_2S Chemistry. For H_2S oxidation and pyrolysis chemistry, the mechanism proposed by Bongartz et al. [39] was used. This mechanism has 157 species and 1011 reactions and was validated for a wide range of conditions including H_2S flame speed measurements, ignition delay times, H_2S pyrolysis, and flow reactor studies. Some validations were also conducted in the presence of methane, which takes into account the sulfur–hydrocarbon species interactions. Since the feed is expected to have only trace amounts of SO_2 or H_2S, this mechanism can yield good results.

2.1.3 NO_x Chemistry. The presence of nitrogen in a combustion chamber results in NO_x formation. Additionally, the presence of nitrogen oxides in hydrocarbon mixtures is known to reduce the time for auto-ignition [40]. To adequately capture NO_x formation and the variations in auto-ignition, we chose the model from Konnov [41]. This mechanism consists of 129 species and 1231 reactions. This mechanism is validated for the ignition delay of hydrocarbon mixtures with NO_x impurities up to 16 atm.

By extracting important reactions for NO_x chemistry and H_2S chemistry from the above mechanisms and merging them with GRI 3.0, a combined reaction mechanism was obtained. This mechanism has 106 species and 916 reactions. This mechanism was used as a base mechanism in this work for generating a sCO_2 combustion mechanism in the presence of NO_x and SO_x impurities.

The base mechanism was optimized using an in-house optimization code written in MATLAB coupled with ANSYS Chemkin Pro [42]. The code edits the rate of constant parameters in the mechanism file and executes Chemkin to run the simulation and provides the mean square error with experimental results. Simulations were conducted using a 0D constant volume closed homogeneous reactor with an energy solver.

Since the final optimized mechanism is expected to retain the performance of individual sub-mechanisms at low pressures, we have limited ourselves to the modification of rates of reactions relevant at high-pressure conditions. The reactions that were chosen to be optimized are shown below:

$$CH_3 + CH_3 \Rightarrow C_2H_6 \quad \text{(R1)}$$

$$C_2H_6 \Rightarrow CH_3 + CH_3 \quad \text{(R1r)}$$

$$C_2H_6 + 2O_2 = 2CH_2O + 2OH \quad \text{(R2)}$$

$$H_2O_2 \Rightarrow 2OH \quad \text{(R3)}$$

Reactions R1 and R1r were chosen since our previous studies on sCO_2 combustion revealed that the recombination reaction of methyl radical plays an important role in supercritical conditions [13]. By including these two reactions in the mechanism, the original methyl radical recombination reaction derived from GRI 3.0 sub-mechanism was removed. The ethane thus formed undergoes a series of reactions that are represented by the lumped reaction R2 to form hydroxyl radicals. The high sensitivity of R3 to ignition delay also made it a target reaction for optimization.

Table 1 Ignition delay data for high-pressure methane combustion at lean and stoichiometric conditions [25]

Mixture composition					
$\phi = 0.5$, CO_2 dilution—86.17%			$\phi = 1$, CO_2 dilution—77.5%		
T (K)	P (atm)	IDT (μs)	T (K)	P (atm)	IDT (μs)
1082	266.8	1098	1045	259.7	636
1086	269.4	1098	1055	245.2	518
1144	262.7	673	1087	249.4	359
1352	75.1	541	1100	285.5	275
1359	78.6	748	1265	109.4	427
1380	74.5	408	1277	111.8	367
1428	73.1	242	1346	34.4	478
1447	35.7	311	1362	103.6	156
1453	72.2	202	1374	27.1	450
1480	32.2	289	1411	100.5	85
1507	27.5	189	1421	32.8	206
1578	30.3	57	1434	35.4	202

Table 2 Ignition delay data for high-pressure hydrogen combustion at lean and stoichiometric conditions [25]

Mixture composition					
$10\%H_2/5\%O_2/85\%CO_2$			$5\%H_2/10\%O_2/85\%CO_2$		
T (K)	P (atm)	IDT (μs)	T (K)	P (atm)	IDT (μs)
1083	251.4	366	1170	40.067	354
1087	275.4	446	1201	39.287	294
1141	244.5	147	1221	37.055	216
1143	311	135	1224	38.204	180
1154	113	258	1270	37.587	90
1161	111	227	–	–	–
1182	110.92	176	–	–	–
1291	103.4	36	–	–	–

Downloaded from http://asmedigitalcollection.asme.org/energyresources/article-pdf/142/12/122302/6543135/jert_142_12_122302.pdf by guest on 28 November 2022

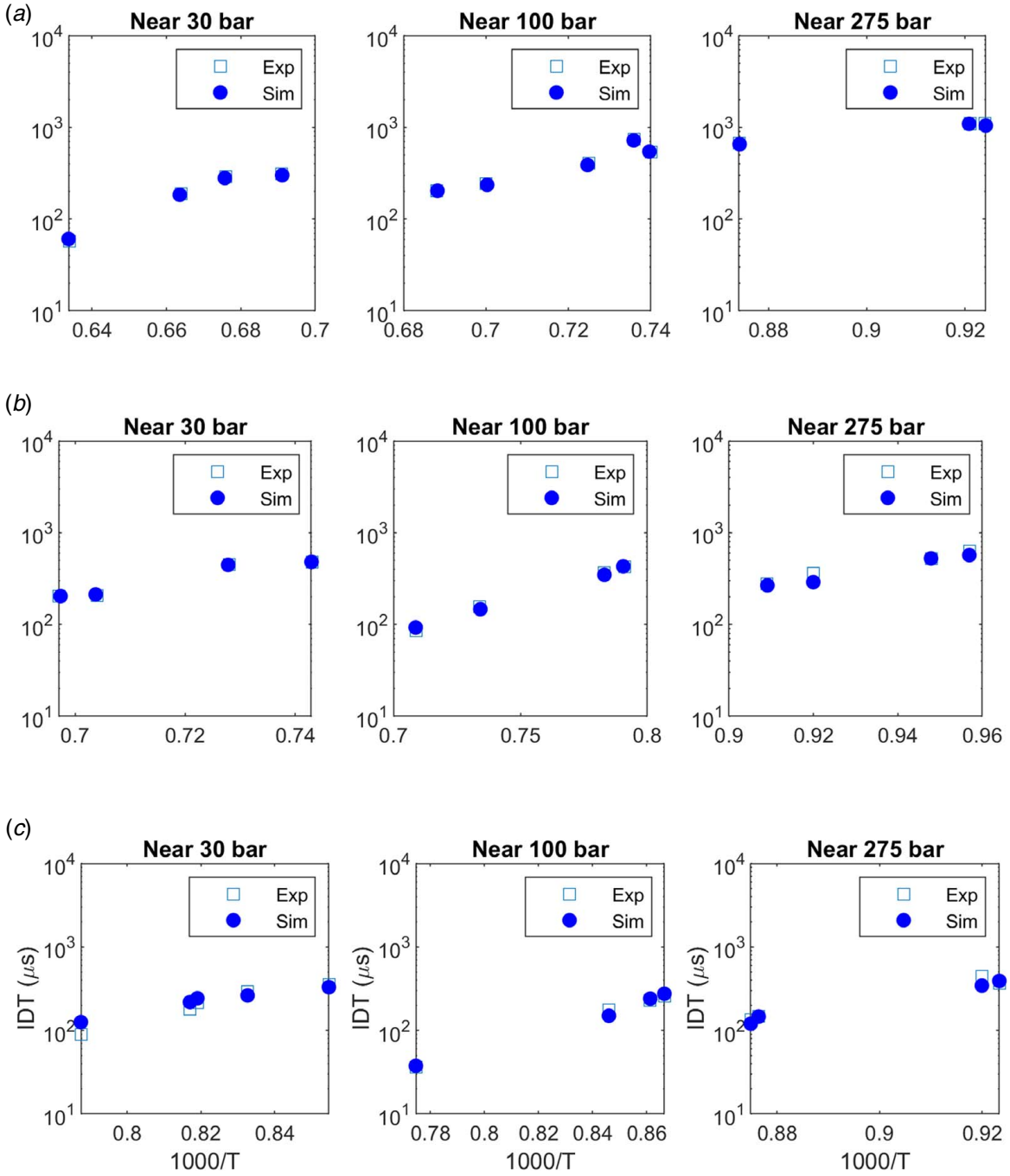

Fig. 1 Results for high-pressure sCO_2 combustion for (*a*) methane oxidation at $\phi = 0.5$, (*b*) methane oxidation at $\phi = 1.0$, and (*c*) hydrogen oxidation at $\phi = 0.25$ at 30 bar and at $\phi = 1$ at 100 and 275 bar. "Exp" is the experimental data from Shao et al. [25] and "Sim" is predictions obtained using optimized model.

3 Shock Tube Experiments

Experiments were conducted in the stainless steel shock tube facility at University of Central Florida (UCF). The shock tube has an inside diameter of 14.17 cm with the driver side separated from the driven section using a metal diaphragm. The test section is located 2.00 cm away from the end section on the driven side. It is equipped with eight optical ports to aid in laser absorption studies. For measuring pressure, one port was installed with a pressure transducer (Kistler 603B1-piezoelectric). Four timer counters (Agilent53220A; 0.1 ns time resolution) were used to measure the time interval, triggered using five piezoelectric transducers (PCB 113B26; 500 kHz frequency response) placed at the last 1.4 m of the driven section. These timer counter values are used to measure the shock velocity, which is then extrapolated linearly to obtain the shock velocity at the end wall. Additional details about shock tube and current experimental strategy are provided in earlier publications [9,11,15,22,23,43–54].

A test mixture was prepared manometrically in a 33-l Teflon-coated stainless steel tank. A fuel mixture (>99.9% purity) identical to natural gas was used, as it is more appropriate for the problem of interest. Argon, oxygen, and CO_2 used were of research grade purity (>99.99%). A 100 Torr (MKS Instruments/Baratron E27D) and 10,000 Torr (MKS Instruments/Baratron 628D) full-scale range capacitance manometers were used to measure the pressure during the filing process. The errors of these manometers were 0.12% and

Downloaded from http://asmedigitalcollection.asme.org/energyresources/article-pdf/142/12/122302/6543135/jert_142_12_122302.pdf by guest on 28 November 2022

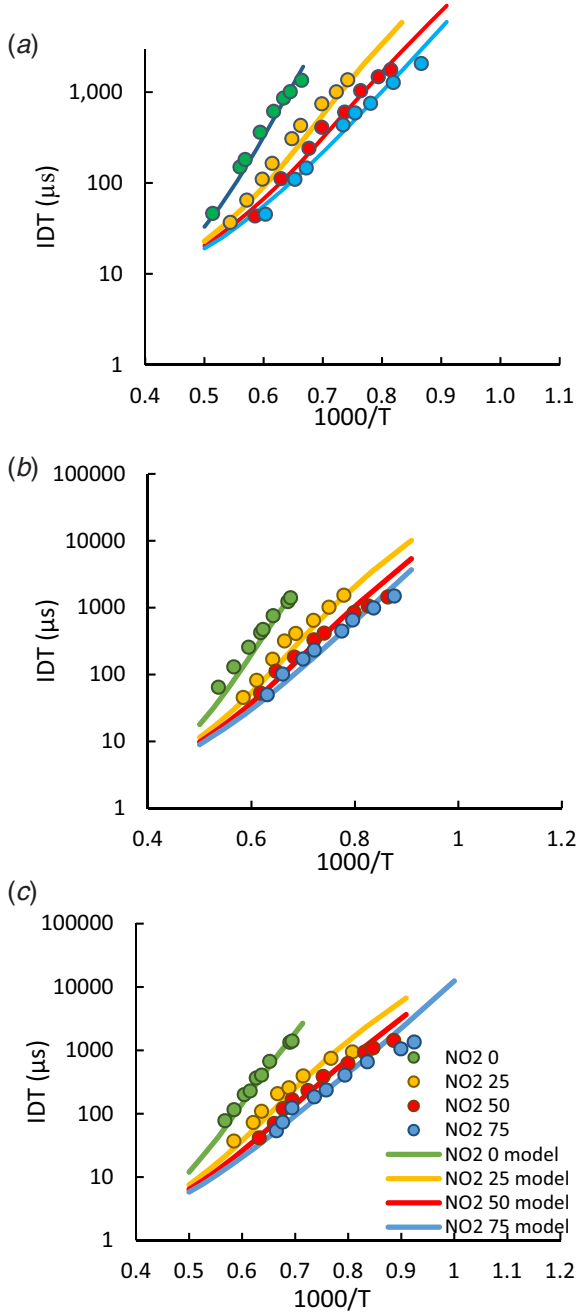

Fig. 2 Comparison between experimental [55] and simulation results for effect of NO_2 impurities on ignition delay of methane at equivalence ratio 1 using the optimized mechanism at (*a*) 5 atm, (*b*) 10 atm, and (c) 16 atm. CH_4 content:1.98%, NO_2 content: NO_2 0–0%, NO_2 25–0.5%, NO_2 50–1% and NO_2 75–1.5%

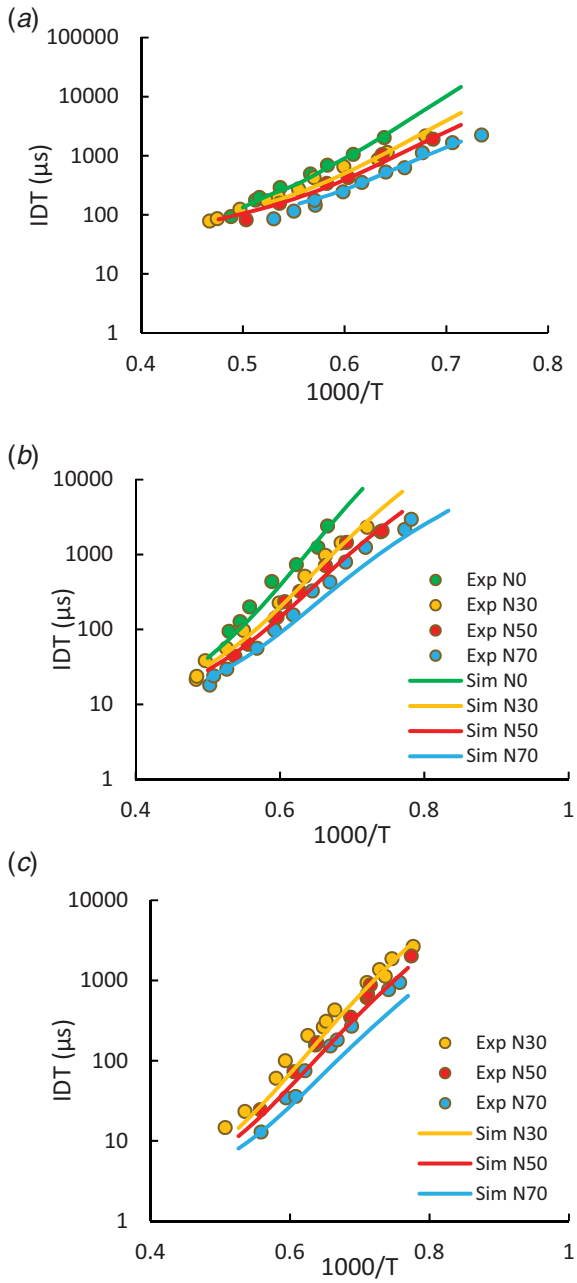

Fig. 3 Comparison between experimental [40] and simulation results for effect of N_2O impurities on ignition delay of methane at equivalence ratio 1 using the optimized mechanism at (*a*) 1.2 atm, (*b*) 4 atm, and (c) 16 atm. Composition of mixtures are N0-1.9%CH_4/3.8%O_2/ Bal Ar, N30-0.8%N_2O/1.9%CH_4/3.8%O_2/ Bal Ar, N50-1.9%N_2O/1.9%CH_4/3.8%O_2/Bal Ar and N70-4.9%N_2O/ 2.0%CH_4/4.1%O_2/Bal Ar.

0.25%, respectively. Helium was used as the driver gas for all experiments. After preparing the mixture, it was stirred for more than 8 h using a magnetically driven stirrer to ensure mixture homogeneity.

4 Results and Discussions

4.1 Mechanism Optimization. The base mechanism generated above has to be optimized for conditions relevant for sCO_2 combustion. For this purpose, the high-pressure experimental data from Shao et al. [25] were used. They conducted shock tube studies at 30–300 bar with methane and hydrogen in high CO_2 dilution. The experimental data considered for lean and stoichiometric oxidation of methane are shown in Table 1. Table 2 shows the ignition delay data for high-pressure combustion of hydrogen at high CO_2 dilution. Data from both Tables 1 and 2 were considered for optimization.

Optimization was performed to minimize the error in predicting experimental results for the temperature range of 1080–1580 K and 1–300 bar. The results obtained using the optimized mechanism is shown in Fig. 1. It can be seen that the optimized mechanism predicts experimental ignition delay times with good accuracy. Optimized reaction mechanism is available upon request from the authors.

Downloaded from http://asmedigitalcollection.asme.org/energyresources/article-pdf/142/12/122302/6543135/jert_142_12_122302.pdf by guest on 28 November 2022

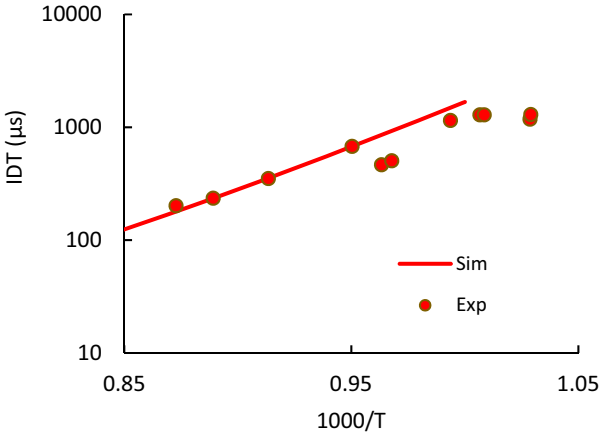

Fig. 4 Comparison between experimental [56] and simulation results for oxidation of H_2S at equivalence ratio of 1.8 at 40 bar. Composition of mixture is 4%H_2S, 6%O_2 and balance argon

4.2 Mechanism Validation. To ensure that the optimized mechanism performs well in predicting any impurity's effect in hydrocarbon combustion, further validations were conducted.

4.2.1 Validation With NO_2 as an Impurity. For validating the effect of NO_2 as an impurity, experimental data were obtained from Zhang et al. [55]. They studied ignition delay of methane in the presence of NO_2 at 5–16 atm in the temperature range of 1100–1900 K. Figure 2 shows the experimental data along with model predictions. It is clear that the mechanism captures the effect of NO_2 on the ignition delay of methane combustion.

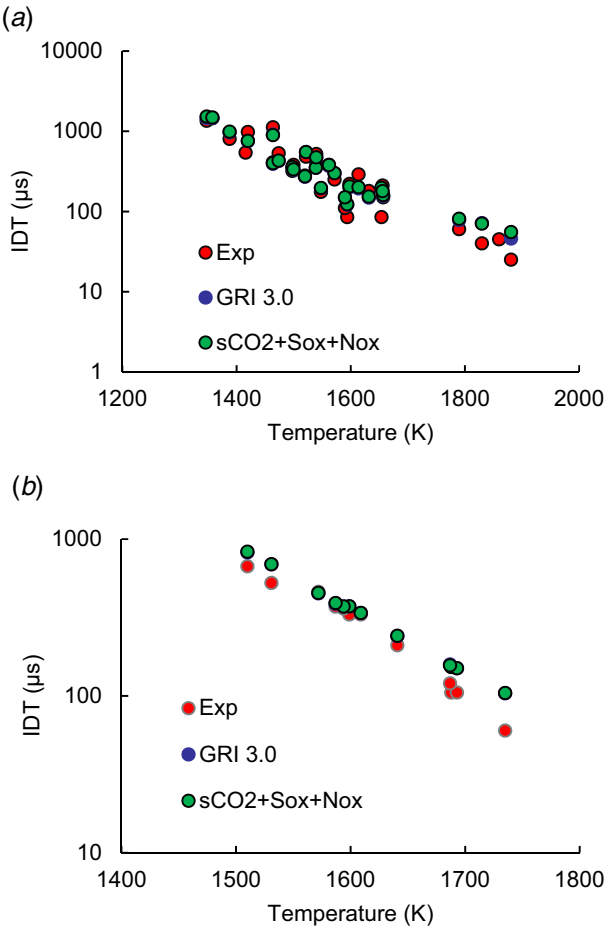

Fig. 5 Comparison between data obtained by Seery and Bowman [57] with GRI 3.0 and model developed in present work ($sCO_2 + SO_x + NO_x$) at (*a*) lean ($\phi = 0.5$) and (*b*) rich ($\phi = 5.0$) conditions. CH_4 content for Φ=5 is 33.3% and Φ=0.5 is 4.8% and inert gas used in experiment was argon.

Table 3 Different mixtures used in shock tube experiments and their compositions in mole fraction

Description	Mixture 1—Without N_2O	Mixture 2—With N_2O
CH_4	0.0157	0.0157
C_2H_6	0.0008	0.0008
C_3H_8	0.0003	0.0003
IC_4H_{10}	0.0001	0.0001
C_4H_{10}	0.0001	0.0001
O_2	0.0362	0.0362
CO_2	0.4470	0.4470
AR	0.4999	0.4899
N_2O	0.0000	0.0100

4.2.2 Validation With N_2O as an Impurity. The effect of small amount of N_2O on ignition delay of methane is studied in Deng et al. [40]. They conducted shock tube studies of methane oxidation at equivalence ratio 0.5 to 2. The experiments were conducted in temperature range of 1220–2336 K and pressure ranging from 1.2 to 16 atm. Figure 3 displays the experimental data along with model predictions for equivalence ratio 1. The results show that the model captures N_2O impurity effect satisfactorily.

4.2.3 Validation for High-Pressure Oxidation of H_2S. To confirm that H_2S oxidation is predicted well by the model, a validation is carried out with the high-pressure oxidation study conducted by Frenklach et al. [56]. The results obtained are shown in Fig. 4. It can be seen that model predicts experimental results very well in the high-temperature region. In the low-temperature regime, a slight deviation is observed.

4.2.4 Validation to Confirm GRI 3.0 Performance. Since the model was optimized only for sCO_2 combustion, it was necessary to confirm whether the mechanism retains GRI 3.0 mechanism performance at low-pressure conditions. Hence, a set of validations were carried out with the works of Seery and Bowman [57]. The results obtained are shown in Fig. 5. It can be seen that the predictions from the present work ($sCO_2 + SO_x + NO_x$) and GRI 3.0 mechanism overlap each other. This confirms that the performance

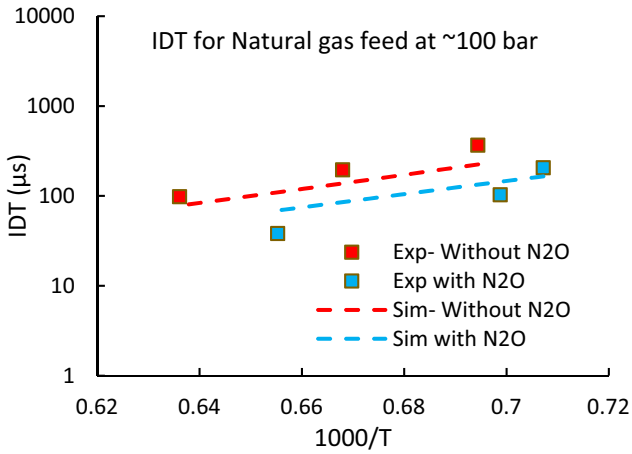

Fig. 6 Experimental results for ignition delay obtained from high-pressure shock tube experiments conducted at UCF. Lines show simulation results using the mechanism developed in this work. See Table 3 for mixture information.

Downloaded from http://asmedigitalcollection.asme.org/energyresources/article-pdf/142/12/122302/6543135/jert_142_12_122302.pdf by guest on 28 November 2022

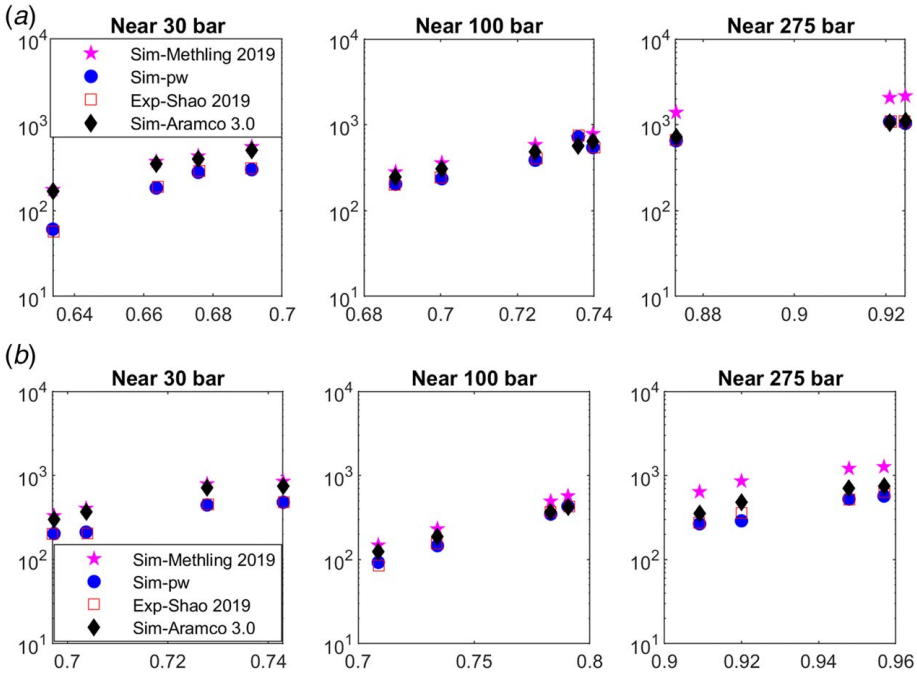

Fig. 7 Comparison with recent mechanisms from literature at high CO_2 dilution and high pressure for methane oxidation at equivalence ratio (*a*) $\phi = 0.5$ and (*b*) $\phi = 1.0$. Experimental data from Shao et al. [25].

of GRI 3.0 mechanism is retained at atmospheric pressure for methane ignition delay.

The Allam cycle sCO_2 combustor has an operating pressure close to 300 bar; therefore, it is necessary to validate the mechanism at pressures close to 300 bar. However, data beyond 17 bar (validation case 1 and 2) were not available in literature for methane ignition delay in presence of impurities. Hence, further experiments are necessary for validating/improving the model.

4.3 Experimental Results and Model Comparison. Experiments were conducted using natural gas feed in the presence and absence of nitrous oxide (N_2O) at pressures in the range of 100–110 bar and temperature of 1400–1580 K. The mixtures used and their compositions are listed in Table 3. In the case of mixture 1, N_2O is replaced with argon. The ignition delay data obtained from experiments are shown in Fig. 6. It can be seen that ignition delay time is faster in the presence of N_2O (the model also predicts faster ignition delay with N_2O).

4.4 Comparison With Recent Mechanisms. The performance of assembled UCF mechanism was compared with two recent mechanisms for natural gas combustion from literature, Aramco mechanism 3.0 [43] and Methling et al. [58] mechanism. Aramco 3.0 has 581 species and 3037 reactions and Methling et al. mechanism have 83 species and 747 reactions. Figure 7 shows the comparison between experimental data from Shao et al. with all the models. At pressure near 30 bar, present model clearly predicts ignition delay better than Aramco 3.0 and Methling et al. models. Near 100 bar, all three models predict ignition delay satisfactorily. At ~275 bar, prediction by Aramco 3.0 and present model are in good agreement with experiments while Methling et al. model overpredicts ignition delay.

4.5 Effect of Impurities on CO Formation. Simulations were conducted in Ansys Chemkin Pro using perfectly stirred reactor model and energy solver. The inlet conditions for "pure methane" simulation were 88.75% CO_2, 3.75% CH_4, and 7.5% O_2. For

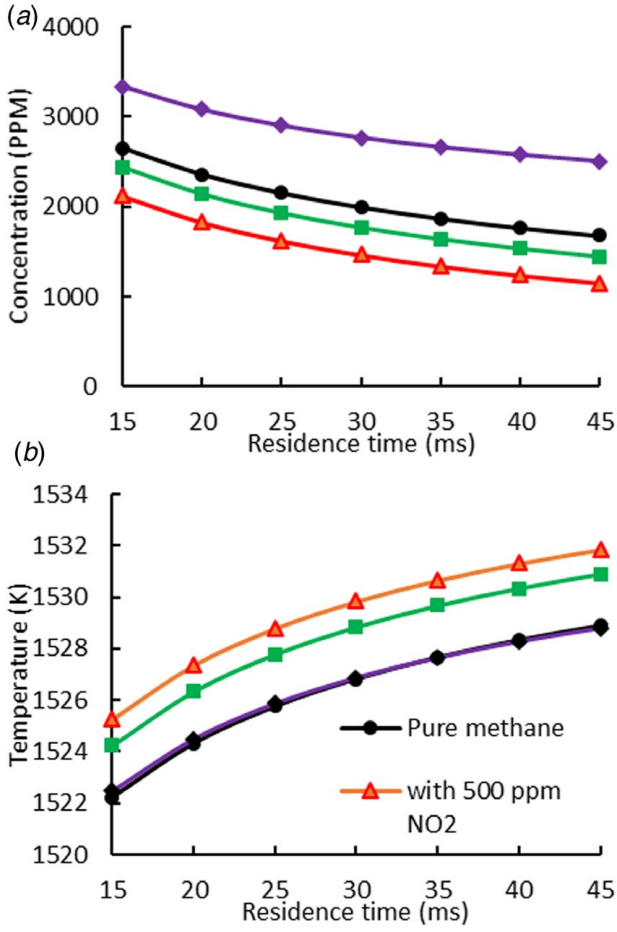

Fig. 8 Simulation results showing the effect of impurities on (*a*) CO formation and (*b*) post-combustion temperature versus residence time

Downloaded from http://asmedigitalcollection.asme.org/energyresources/article-pdf/142/12/122302/6543135/jert_142_12_122302.pdf by guest on 28 November 2022

simulations with impurities, 0.05% of CO_2 was replaced with the corresponding impurity. The inlet temperature and pressure were 1000 K and 300 bar, respectively, which resulted in a post-combustion temperature close to 1500 K. Figure 8(*a*) shows the CO concentration versus residence time with 500 ppm of NO_2, N_2O, and H_2S as impurities. The presence of trace amount of N_2O and NO_2 reduces the amount of CO produced during sCO_2 combustion. On the contrary, H_2S presents as an impurity resulted in production of more CO. The higher post-combustion temperatures observed (Fig. 8(*b*)) for cases with N_2O and NO_2 can be attributed to the efficient conversion of CO to CO_2. However, no significant reduction in post-combustion temperature was observed in presence of H_2S as impurity even with considerable increase in CO production. This can be attributed to the energy release from H_2S oxidation balancing the reduction in energy due to CO formation.

5 Conclusions

In this work, we developed a detailed reaction mechanism for sCO_2 combustion in the presence of NO_x and SO_x impurities. The developed mechanism was validated extensively with data obtained from the literature. Validations were carried out to check whether the mechanism captured the impurity effects of NO_x. It was observed that the mechanism was able to capture the impurity effect of NO_x on ignition delay time up to 17 bar. Since further validation targets at higher pressure were not available in literature, we conducted experiments using natural gas identical mixture at UCF's shock tube facility to study the effect of N_2O at 100 bar. Results obtained indicated that faster ignition delay time was observed for this mixture in the presence of N_2O (when compared with ignition delay time measured without N_2O). These results were then used as validation target for the model; good agreement was observed. The generated reaction mechanism was used to predict CO formation from sCO_2 combustor in presence of impurities. It was observed that presence of NO_x impurities helped in reducing CO while H_2S increased CO formation. The reaction mechanism presented here can be used as a base mechanism to generate reduced mechanisms for CFD simulations.

Acknowledgment

This material is mainly based upon work supported by the U.S. Department of Energy, Office of Science, Office of Basic Energy Sciences under Award Number DE-SC0019640. Also, this material is partially supported by the U.S. Department of Energy under award numbers DE-FE0025260 and DE-EE0007982.

Disclaimer

This report was prepared as an account of work sponsored by an agency of the United States Government. Neither the United States Government nor any agency thereof, nor any of their employees, makes any warranty, express or implied, or assumes any legal liability or responsibility for the accuracy, completeness, or usefulness of any information, apparatus, product, or process disclosed, or represents that its use would not infringe privately owned rights. Reference herein to any specific commercial product, process, or service by trade name, trademark, manufacturer, or otherwise does not necessarily constitute or imply its endorsement, recommendation, or favoring by the United States Government or any agency thereof. The views and opinions of authors expressed herein do not necessarily state or reflect those of the United States Government or any agency thereof.

Conflict of Interest

There are no conflicts of interest.

References

[1] Allam, R., Fetvedt, J., Forrest, B., and Freed, D., "The Oxy-Fuel, Supercritical CO2 Allam Cycle: New Cycle Developments to Produce Even Lower-Cost Electricity From Fossil Fuels Without Atmospheric Emissions," Proceedings of the ASME Turbo Expo 2014: Turbine Technical Conference and Exposition, American Society of Mechanical Engineers, p. V03BT36A016.

[2] Vesely, L., Manikantachari, K. R. V., Vasu, S., Kapat, J., Dostal, V., and Martin, S., 2018, "Effect of Impurities on Compressor and Cooler in Supercritical CO2 Cycles," ASME J. Energy Resour. Technol., **141**(1), p. 012003.

[3] Khadse, A., Blanchette, L., Kapat, J., Vasu, S., Hossain, J., and Donazzolo, A., 2018, "Optimization of Supercritical CO2 Brayton Cycle for Simple Cycle Gas Turbines Exhaust Heat Recovery Using Genetic Algorithm[Q7] Turbines Exhaust Heat Recovery Using Genetic Algorithm," ASME J. Energy Resour. Technol., **140**(7), p. 071601.

[4] Black, J., Straub, D., Robey, E., Yip, J., Ramesh, S., Roy, A., and Searle, M., 2020, "Measurement of Convective Heat Transfer Coefficients With Supercritical CO2 Using the Wilson-Plot Technique," ASME J. Energy Resour. Technol., **142**(7), p. 070901.

[5] Deshmukh, A., and Kapat, J., 2020, "Pinch Point Analysis of Air Cooler in Supercritical Carbon Dioxide Brayton Cycle Operating Over Ambient Temperature Range," ASME J. Energy Resour. Technol., **142**(5), p. 050509.

[6] Fang, L., Li, Y., Yang, X., and Yang, Z., 2019, "Analyses of Thermal Performance of Solar Power Tower Station Based on a Supercritical CO2 Brayton Cycle," ASME J. Energy Resour. Technol., **142**(3), p. 031301.

[7] Bai, Z., Zhang, G., Yang, Y., and Wang, Z., 2019, "Design Performance Simulation of a Supercritical CO2 Cycle Coupling With a Steam Cycle for gas Turbine Waste Heat Recovery," ASME J. Energy Resour. Technol., **141**(10), p. 102001.

[8] Pryor, O. M., Vasu, S., Lu, X., Freed, D., and Forrest, B., 2018, "Development of a Global Mechanism for Oxy-Methane Combustion in a CO2 Environment," (51180), p. V009T038A004.

[9] Pryor, O. M., Barak, S., Koroglu, B., Ninnemann, E., and Vasu, S. S., 2017, "Measurements and Interpretation of Shock Tube Ignition Delay Times in Highly CO2 Diluted Mixtures Using Multiple Diagnostics," Combust. Flame, **180**, pp. 63–76.

[10] Pryor, O., Koroglu, B., Barak, S., Lopez, J., Ninnemann, E., Nash, L., and Vasu, S., 2017, "Ignition Delay Times of High Pressure Oxy-Methane Combustion With High Levels of CO2 Dilution," (50848), p. V04AT04A044.

[11] Pryor, O., Barak, S., Lopez, J., Ninnemann, E., Koroglu, B., Nash, L., and Vasu, S., 2017, "High Pressure Shock Tube Ignition Delay Time Measurements During Oxy-Methane Combustion With High Levels of CO2 Dilution," ASME J. Energy Resour. Technol., **139**(4), p. 042208.

[12] Vasu, S. S., Pryor, O. M., Kapat, J. S., Masunov, A., and Martin, S. M., 2016, "Developing a Validated Chemical Kinetics Model for sCO2 Combustion and Implementation in CFD," Proceedings of the Supercritical CO2 Power Cycles Symposium, San Antonio, TX, Paper#7.

[13] Wang, C.-H., Panteleev, S. V., Masunov, A. E., Allison, T. C., Chang, S., Lim, C., Jin, Y., and Vasu, S. S., 2019, "Molecular Dynamics of Combustion Reactions in Supercritical Carbon Dioxide. Part 5: Computational Study of Ethane Dissociation and Recombination Reactions C2H6 ⇌ CH3 + CH3," J. Phys. Chem. A, **123**(22), pp. 4776–4784.

[14] Manikantachari, K. R. V., Martin, S., Rahman, R. K., Velez, C., and Vasu, S., 2019, "A General Study of Counterflow Diffusion Flames for Supercritical CO2 Combustion," ASME J. Eng. Gas Turbines Power, **141**(12), p. 121020.

[15] Barak, S., Pryor, O., Ninnemann, E., Neupane, S., Vasu, S., Lu, X., and Forrest, B., 2020, "Ignition Delay Times of Oxy-Syngas and Oxy-Methane in Supercritical CO2 Mixtures for Direct-Fired Cycles," ASME J. Eng. Gas Turbines Power, **142**(2), p. 021014.

[16] Manikantachari, K. R. V., Martin, S., Bobren-Diaz, J. O., and Vasu, S., 2017, "Thermal and Transport Properties for the Simulation of Direct-Fired sCO2 Combustor," ASME J. Eng. Gas Turbines Power, **139**(12), p. 121505.

[17] Naik, C. V., Puduppakkam, K. V., and Meeks, E., 2019, "A Comprehensive Kinetics Library for Simulating the Combustion of Automotive Fuels," ASME J. Energy Resour. Technol., **141**(9), p. 092201.

[18] Manikantachari, K. R. V., Vesely, L., Martin, S., Bobren-Diaz, J. O., and Vasu, S., 2018, "Reduced Chemical Kinetic Mechanisms for Oxy/Methane Supercritical CO2 Combustor Simulations," ASME J. Energy Resour. Technol., **140**(9), p. 092202.

[19] Yelishala, S. C., Wang, Z., Metghalchi, H., Levendis, Y. A., Kannaiyan, K., and Sadr, R., 2019, "Effect of Carbon Dioxide on the Laminar Burning Speed of Propane–Air Mixtures," ASME J. Energy Resour. Technol., **141**(8), p. 082205.

[20] Wang, Z., Yelishala, S. C., Yu, G., Metghalchi, H., and Levendis, Y. A., 2019, "Effects of Carbon Dioxide on Laminar Burning Speed and Flame Instability of Methane/Air and Propane/Air Mixtures: A Literature Review," Energy Fuels, **33**(10), pp. 9403–9418.

[21] Vasu, S. S., Davidson, D. F., and Hanson, R. K., 2011, "Shock Tube Study of Syngas Ignition in Rich CO2 Mixtures and Determination of the Rate of H+ O2+ CO2→ HO2+ CO2," Energy Fuels, **25**(3), pp. 990–997.

[22] Koroglu, B., Neupane, S., Pryor, O., Peale, R. E., and Vasu, S. S., 2018, "High Temperature Infrared Absorption Cross Sections of Methane Near 3.4 μm in Ar and CO2 Mixtures," J. Quantitative Spectrosc. Radiative Transfer, **206**(Suppl C), pp. 36–45.

[23] Koroglu, B., Pryor, O., Lopez, J., Nash, L., and Vasu, S. S., 2016, "Shock Tube Ignition Delay Times and Methane Time-Histories Measurements During Excess CO2 Diluted Oxy-Methane Combustion," Combust. Flame, **164**, pp. 152–163.

Downloaded from http://asmedigitalcollection.asme.org/energyresources/article-pdf/142/12/122302/6543135/jert_142_12_122302.pdf by guest on 28 November 2022

[24] Askari, O., Vien, K., Wang, Z., Sirio, M., and Metghalchi, H., 2016, "Exhaust gas Recirculation Effects on Flame Structure and Laminar Burning Speeds of H2/CO/air Flames at High Pressures and Temperatures," Appl. Energy, **179**, pp. 451–462.
[25] Shao, J., Choudhary, R., Davidson, D. F., Hanson, R. K., Barak, S., and Vasu, S., 2019, "Ignition Delay Times of Methane and Hydrogen Highly Diluted in Carbon Dioxide at High Pressures up to 300 atm," Proc. Combust. Inst., **37**(4), pp. 4555–4562.
[26] Barak, S., Pryor, O., Ninnemann, E., Neupane, S., Lu, X., Forrest, B., and Vasu, S., "Ignition Delay Times of Syngas and Methane in sCO2 Diluted Mixtures for Direct-Fired Cycles," Proceedings of the ASME Turbo Expo 2019: Turbomachinery Technical Conference and Exposition, p. V009T38A001.
[27] Li, Y., Zhou, C.-W., Somers, K. P., Zhang, K., and Curran, H. J., 2017, "The Oxidation of 2-Butene: A High Pressure Ignition Delay, Kinetic Modeling Study and Reactivity Comparison With Isobutene and 1-Butene," Proc. Combust. Inst., **36**(1), pp. 403–411.
[28] Wait, E. E., Masunov, A. E., and Vasu, S. S., 2019, "Quantum Chemical and Master Equation Study of OH + CH2O → H2O + CHO Reaction Rates in Supercritical CO2 Environment," Int. J. Chem. Kinet., **51**(1), pp. 42–48.
[29] Panteleev, S. V., Masunov, A. E., and Vasu, S. S., 2019, "Molecular Dynamics of Combustion Reactions in Supercritical Carbon Dioxide. Part 4: Boxed MD Study of Formyl Radical Dissociation and Recombination," J. Mol. Mod., **25**(2), p. 35.
[30] Masunov, A. E., Wait, E. E., and Vasu, S. S., 2018, "Catalytic Effect of Carbon Dioxide on Reaction OH + CO → H + CO2 in Supercritical Environment: Master Equation Study," J. Phys. Chem. A, **122**(31), pp. 6355–6359.
[31] Masunov, A. E., Wait, E. E., Atlanov, A. A., and Vasu, S. S., 2017, "Quantum Chemical Study of Supercritical Carbon Dioxide Effects on Combustion Kinetics," J. Phys. Chem. A, **121**(19), pp. 3728–3735.
[32] Masunov, A. E., Wait, E., and Vasu, S. S., 2017, "Quantum Chemical Study of CH3 + O2 Combustion Reaction System: Catalytic Effects of Additional CO2 Molecule," J. Phys. Chem. A, **121**(30), pp. 5681–5689.
[33] Masunov, A. E., Wait, E., and Vasu, S. S., 2016, "Chemical Reaction CO + OH• → CO2+H• Autocatalyzed by Carbon Dioxide: Quantum Chemical Study of the Potential Energy Surfaces," J. Phys. Chem. A, **120**(30), pp. 6023–6028.
[34] Masunov, A. E., Atlanov, A. A., and Vasu, S. S., 2016, "Molecular Dynamics Study of Combustion Reactions in a Supercritical Environment. Part 1: Carbon Dioxide and Water Force Field Parameters Refitting and Critical Isotherms of Binary Mixtures," Energy Fuels, **30**(11), pp. 9622–9627.
[35] Masunov, A. E., Atlanov, A. A., and Vasu, S. S., 2016, "Potential Energy Surfaces for the Reactions of HO2 Radical With CH2O and HO2 in CO2 Environment," J. Phys. Chem. A, **120**(39), pp. 7681–7688.
[36] Wang, C.-H., Masunov, A. E., Allison, T. C., Chang, S., Lim, C., Jin, Y., and Vasu, S. S., 2019, "Molecular Dynamics of Combustion Reactions in Supercritical Carbon Dioxide. 6. Computational Kinetics of Reactions Between Hydrogen Atom and Oxygen Molecule H + O2 ⇌ HO + O and H + O2 ⇌ HO2," J. Phys. Chem. A, **123**(50), pp. 10772–10781.
[37] Panteleev, S. V., Masunov, A. E., and Vasu, S. S., 2018, "Molecular Dynamics Study of Combustion Reactions in a Supercritical Environment. Part 2: Boxed MD Study of CO + OH → CO2 + H Reaction Kinetics," J. Phys. Chem. A, **122**(4), pp. 897–908.
[38] Smith, G. P., Michael Frenklach, D. M. G., Moriarty, N. W., Eiteneer, B., Goldenberg, M., Thomas Bowman, C., Hanson, R. K., Song, S., Gardiner, W. C., Jr., Lissianski, V. V., and Qin, Z., http://combustion.berkeley.edu/gri_mech/.
[39] Bongartz, D., and Ghoniem, A. F., 2015, "Chemical Kinetics Mechanism for Oxy-Fuel Combustion of Mixtures of Hydrogen Sulfide and Methane," Combust. Flame, **162**(3), pp. 544–553.
[40] Deng, F., Yang, F., Zhang, P., Pan, Y., Zhang, Y., and Huang, Z., 2016, "Ignition Delay Time and Chemical Kinetic Study of Methane and Nitrous Oxide Mixtures at High Temperatures," Energy Fuels, **30**(2), pp. 1415–1427.
[41] Konnov, A. A., 2009, "Implementation of the NCN Pathway of Prompt-NO Formation in the Detailed Reaction Mechanism," Combust. Flame, **156**(11), pp. 2093–2105.
[42] 2019, "ANSYS Chemkin-Pro," http://www.ansys.com/products/fluids/ansys-chemkin-pro, San Diego, CA.
[43] Zhou, C.-W., Li, Y., Burke, U., Banyon, C., Somers, K. P., Ding, S., Khan, S., Hargis, J. W., Sikes, T., Mathieu, O., Petersen, E. L., AlAbbad, M., Farooq, A., Pan, Y., Zhang, Y., Huang, Z., Lopez, J., Loparo, Z., Vasu, S. S., and Curran, H. J., 2018, "An Experimental and Chemical Kinetic Modeling Study of 1,3-Butadiene Combustion: Ignition Delay Time and Laminar Flame Speed Measurements," Combust. Flame, **197**, pp. 423–438.
[44] Barak, S., Ninnemann, E., Neupane, S., Barnes, F., Kapat, J., and Vasu, S., 2018, "High-Pressure Oxy-Syngas Ignition Delay Times With CO2 Dilution: Shock Tube Measurements and Comparison of the Performance of Kinetic Mechanisms," ASME J. Eng. Gas Turbines Power, **141**(2), pp. 021011–021017.
[45] Loparo, Z. E., Lopez, J. G., Neupane, S., Partridge, W. P., Vodopyanov, K., and Vasu, S. S., 2017, "Fuel-Rich n-Heptane Oxidation: A Shock Tube and Laser Absorption Study," Combust. Flame, **185**(Supplement C), pp. 220–233.
[46] Barak, S., Pryor, O., Lopez, J., Ninnemann, E., Vasu, S., and Koroglu, B., 2017, "High-Speed Imaging and Measurements of Ignition Delay Times in Oxy-Syngas Mixtures With High CO2 Dilution in a Shock Tube," ASME J. Eng. Gas Turbines Power, **139**(12), p. 121503.
[47] Loparo, Z. E., Muraviev, A. V., Figueiredo, P., Lyakh, A., Peale, R. E., Ahmed, K., and Vasu, S. S., 2018, "Shock Tube Demonstration of Acousto-Optically Modulated Quantum Cascade Laser as a Broadband, Time-Resolved Combustion Diagnostic," ASME J. Energy Resour. Technol., **140**(11), p. 112202.
[48] Koroglu, B., and Vasu, S. S., 2016, "Measurements of Propanal Ignition Delay Times and Species Time Histories Using Shock Tube and Laser Absorption," Int. J. Chem. Kinet., **48**(11), pp. 679–690.
[49] Barari, G., Pryor, O., Koroglu, B., Sarathy, S. M., Masunov, A. E., and Vasu, S. S., 2017, "High Temperature Shock Tube Experiments and Kinetic Modeling Study of Diisopropyl Ketone Ignition and Pyrolysis," Combust. Flame, **177**, pp. 207–218.
[50] Loparo, Z. E., Ninnemann, E., Thurmond, K., Laich, A., Azim, A., Lyakh, A., and Vasu, S. S., 2019, "Acousto-Optically Modulated Quantum Cascade Laser for High-Temperature Reacting Systems Thermometry," Opt. Lett., **44**(6), pp. 1435–1438.
[51] Ninnemann, E., Kim, G., Laich, A., Almansour, B., Terracciano, A. C., Park, S., Thurmond, K., Neupane, S., Wagnon, S., Pitz, W. J., and Vasu, S. S., 2019, "Co-optima Fuels Combustion: A Comprehensive Experimental Investigation of Prenol Isomers," Fuel, **254**, p. 115630.
[52] Barak, S., Rahman, R. K., Neupane, S., Ninnemann, E., Arafin, F., Laich, A., Terracciano, A. C., and Vasu, S. S., 2020, "Measuring the Effectiveness of High-Performance Co-Optima Biofuels on Suppressing Soot Formation at High Temperature," Proc. Natl. Acad. Sci. U. S. A., **117**(7), pp. 3451–3460.
[53] Loparo, Z. E., Ninnemann, E., Ru, Q., Vodopyanov, K. L., and Vasu, S. S., 2020, "Broadband Mid-Infrared Optical Parametric Oscillator for Dynamic High-Temperature Multi-Species Measurements in Reacting Systems," Opt. Lett., **45**(2), pp. 491–494.
[54] Neupane, S., Rahman, R. K., Baker, J., Arafin, F., Ninnemann, E., Thurmond, K., Wang, C.-H., Masunov, A. E., and Vasu, S. S., 2020, "DMMP Pyrolysis and Oxidation Studies at High Temperature Inside a Shock Tube Using Laser Absorption Measurements of CO," Combust. Flame, **214**, pp. 14–24.
[55] Zhang, X., Ye, W., Shi, J. C., Wu, X. J., Zhang, R. T., and Luo, S. N., 2017, "Shock-Induced Ignition of Methane, Ethane, and Methane/Ethane Mixtures Sensitized by NO2," Energy Fuels, **31**(11), pp. 12780–12790.
[56] Frenklach, M., Lee, J. H., White, J. N., and Gardiner, W. C., 1981, "Oxidation of Hydrogen Sulfide," Combust. Flame, **41**, pp. 1–16.
[57] Seery, D. J., and Bowman, C. T., 1970, "An Experimental and Analytical Study of Methane Oxidation Behind Shock Waves," Combust. Flame, **14**(1), pp. 37–47.
[58] Methling, T., Braun-Unkhoff, M., and Riedel, U., 2019, "An Optimised Chemical Kinetic Model for the Combustion of Fuel Mixtures of Syngas and Natural gas," Fuel, **262**, p. 116611.

Downloaded from http://asmedigitalcollection.asme.org/energyresources/article-pdf/142/12/122302/6543135/jert_142_12_122302.pdf by guest on 28 November 2022